

CHAPTER 13

Near-Critical Micellization for Nanomedicine: Enhanced Drug Loading, Reduced Burst Release

JADE GREEN^a, MACIEJ RADOSZ^{*a} AND
YOUQING SHEN^b

^a Department of Chemical and Petroleum Engineering, Soft Materials Laboratory, University of Wyoming, Laramie, WY 82071, USA; ^b Center for Bionanoengineering and State Key Laboratory of Chemical Engineering, Department of Chemical and Biological Engineering, Zhejiang University, Hangzhou 310027, P. R. China

*E-mail: Radosz@uwyo.edu

13.1 Introduction

Micelles, a self-assembled formation of diblock copolymer chains, have been shown to have utility for delivery of highly hydrophobic drugs.^{1–5} This is due to their ability to solubilize these drugs into the core of the micelle, thereby increasing the effective dose of drug available for delivery, and to target cancer cells *via* the enhanced permeation and retention (EPR) effect.^{6–8} In most conventional methods, such diblock micelles are formed by first dissolving the copolymer in a nonselective solvent, such as acetone. Then, micelle formation is induced by the slow addition of a selective solvent, such as water. Finally, the micelles are removed and purified by freeze drying, solvent evaporation, or dialysis.^{8–11} However, there are problems associated with such methods,

including trace amounts of potentially toxic organic solvents left in the micelle, low drug loading, and burst release of the drug, to name a few.

We recently developed a new technology that can address these problems by using a near-critical solvent, which is a compressed gas, and simply reducing the pressure to induce micellization, referred to as the near-critical micellization (NCM) method. In addition to low viscosity and high diffusivity, which promote mass transfer, near-critical solvents are easy to remove by spontaneous and complete evaporation. More importantly, solvent capacity and selectivity can be tuned precisely with its density *via* pressure, temperature, or both, which, in contrast to liquid solvents, allows for high-resolution control of the NCM process.^{8,12}

13.2 Early Feasibility Studies on Model Systems

The first step in developing the NCM process was to understand its physics on simple, well-defined model systems, such as polystyrene and polyisoprene. Towards this end, Winoto *et al.*¹³ used an experimental set-up shown in Figure 13.1, in which a small high-pressure, variable-volume ($\sim 1 \text{ cm}^3$) cell is used to detect cloud pressure (CP) and micellization pressure (MP) transitions. It is equipped with a floating piston, so that the pressure can be changed

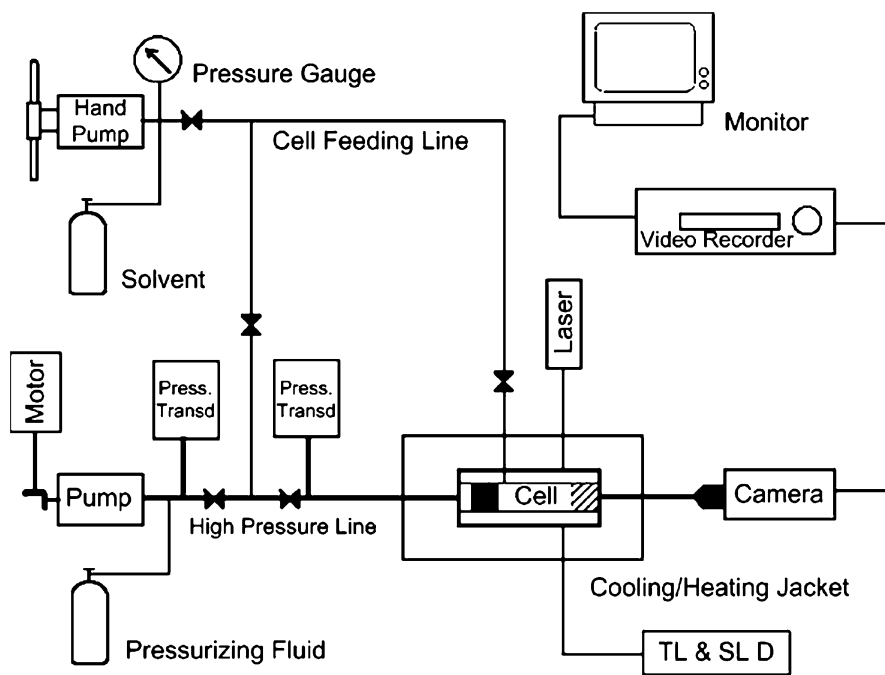


Figure 13.1 A simplified apparatus schematic diagram. (Reproduced from Winoto *et al.*¹³ with permission from the American Chemical Society.)

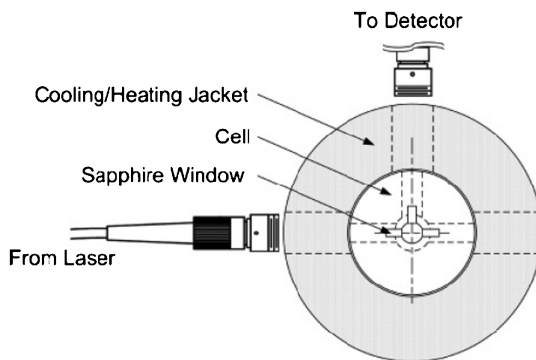


Figure 13.2 The optical fiber interface with the cell. (Reproduced from Winoto *et al.*¹³ with permission from the American Chemical Society.)

without changing the mixture composition. It also has a borescope for visual observation of the phase transitions, and transmitted- and scattered-light intensity probes, arranged as shown in Figure 13.2. The apparatus is also equipped with a data-acquisition system that allows for measurements at constant pressure and temperature and for increasing and decreasing the pressure and temperature at constant rate. The CP is detected by a transmitted-light intensity (TLI) probe, which measures light at 180° from the laser. The MP is detected using a scattered-light intensity (SLI) probe, which is measured at 90° from the laser.

The CP at a given temperature is the specific pressure at which the capacity of the solvent is just enough to allow complete dissolution of the polymer. Above the CP, the polymer is dissolved. Below the CP, the polymer forms a distinct separate phase, at the onset of which the solution becomes opaque, or “cloudy.” Similarly, for block copolymers the MP at a given temperature is the specific pressure at which solvent selectivity forces the less-soluble block to aggregate as the micelle cores. In the micellar region, below the MP but above the CP, a micellar solution exists as a result of nano, rather than bulk, phase separation. At pressures above the MP, the solvent is no longer selective enough to induce solvent-phobic block aggregation, so the micelles cease to exist.

In a typical experiment, a known amount of copolymer is loaded into the cell and pressurized with a known amount of solvent, both obtained by weighing the cell. Following weighing, the cell is brought to and maintained at a desired pressure and temperature to dissolve the copolymer completely and left, stirred, in the one-phase region for about 90 min to reach equilibrium.

To obtain a CP data point, the pressure is lowered slowly until the solution becomes cloudy at the onset of bulk phase separation, which is indicated by a drop in TLI. Pressure drop rates as low as 15 bar min^{-1} are used to obtain a reproducible CP, to within 3 bar. The bulk phase boundary can also be

approached from the two-phase side upon compression, which leads to an increase in TLI, but produces roughly the same result, with no significant hysteresis. The solution is allowed to equilibrate in the one-phase region at a much higher pressure than the expected CP for 15 min before a new data point is taken. For all data points, the TLI results are stored and analyzed as a function of temperature, pressure, and time.

Since the SLI and hydrodynamic radius increase sharply at the MP, micelle formation can be measured using high-pressure dynamic light scattering. For these measurements, the high-pressure cell is coupled with an Ar⁺ ion laser (National Laser, model 800BL) operating at a $\lambda = 488$ nm wavelength with a Brookhaven BI-9000AT correlator. The coherence area is controlled by a pinhole placed before the detector. The laser and detector are linked to the high-pressure cell by optical fibers produced by Thorlabs. The high-pressure optical interface design is different from, but inspired by, the approach described by Koga *et al.*³ The scattered-light intensity is recorded and measured for isothermal measurements upon increasing or decreasing pressures at a rate of 30–60 bar min⁻¹. More detailed descriptions are available elsewhere.^{13–15}

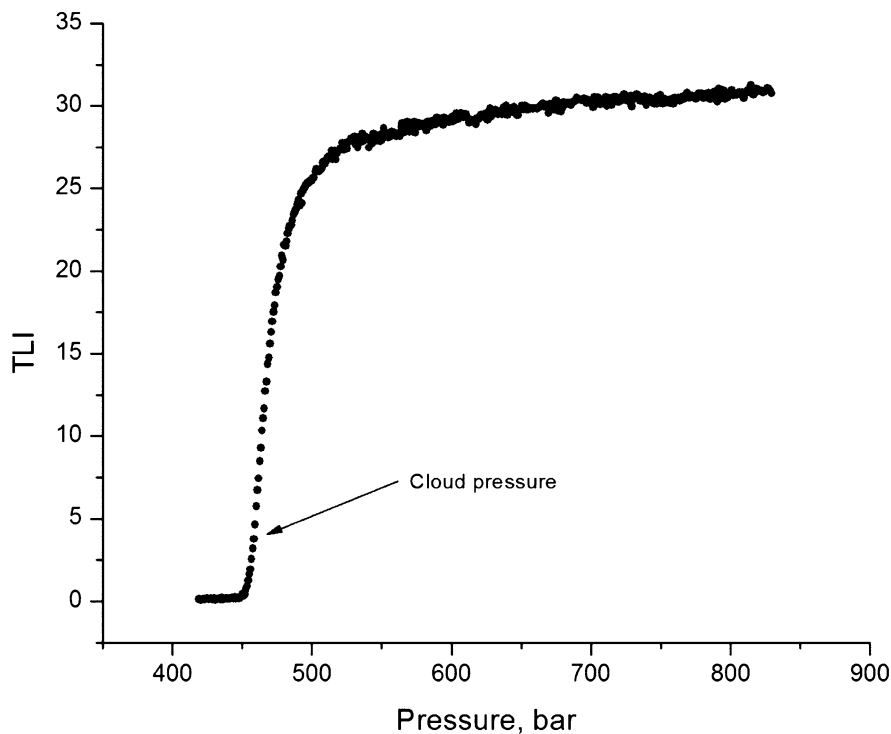


Figure 13.3 Transmitted light intensity plot of PEG-b-PCL (5k-b-11k) in 33% trifluoromethane and 67% dimethyl ether at 40 °C and 1 wt%.

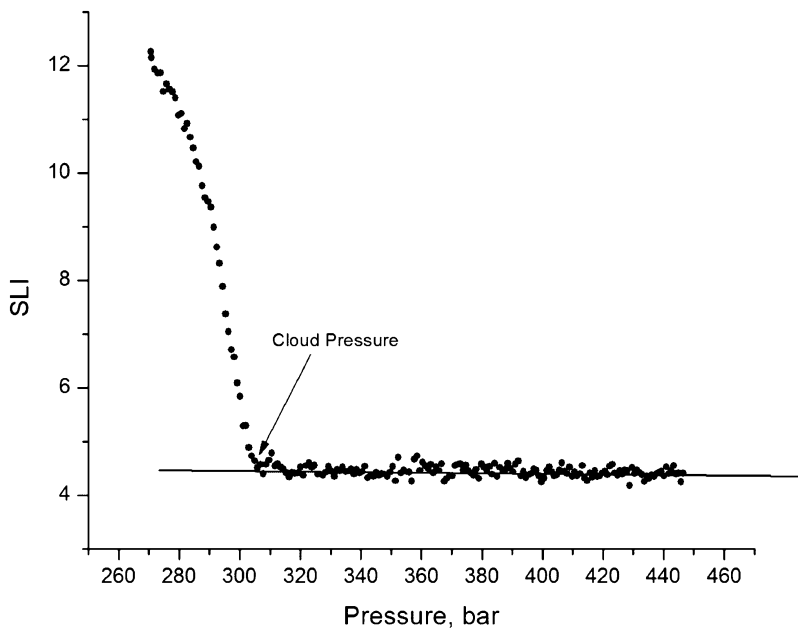


Figure 13.4 Scattered light intensity plot (without micellization) of PEG-*b*-PCL (5k-*b*-11k) in dimethyl ether at 100 °C and 1 wt%.

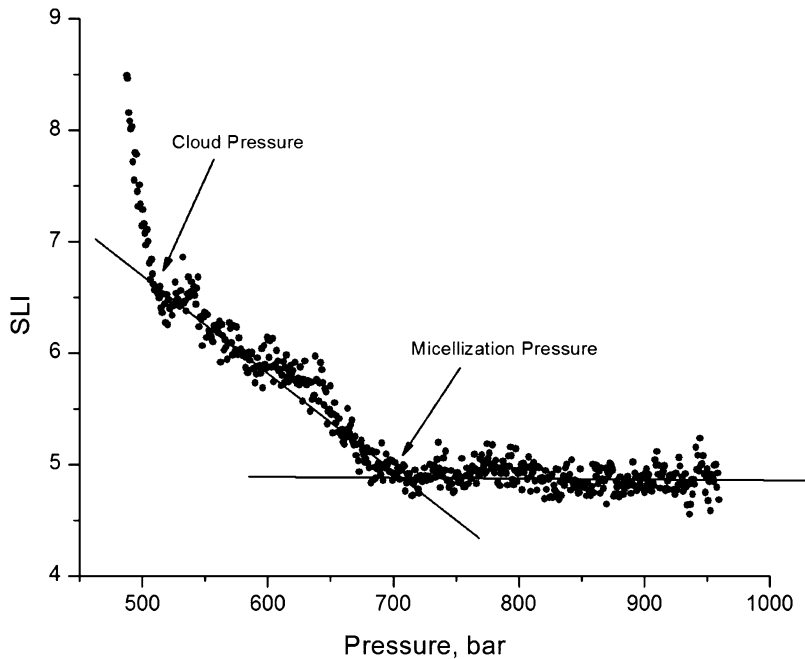


Figure 13.5 Scattered light intensity plot (with micellization) of PEG-*b*-PCL (5k-*b*-11k) in 33% trifluoromethane and 67% dimethyl ether at 60 °C and 1 wt%.

Figure 13.3 shows a sample graph of the TLI as a function of pressure. The CP is determined to be the inflection point of the TLI curve, which corresponds to a peak in its first derivative. Sample graphs of two typical cases of SLI curves are shown in Figures 13.4 and 13.5. Figure 13.4 illustrates an example with no micellization; the SLI increases sharply at the CP, but remains constant until then. By contrast, Figure 13.5 illustrates an example with micellization, where upon decreasing pressure, the SLI starts increasing at the MP, and then increases sharply at the CP.

A complete example of those early feasibility studies by Winoto *et al.*¹³ is shown in Figure 13.6 for 0.5 wt% polystyrene-*block*-polyisoprene (MW 11.5k-*b*-10.5k) in propane. As explored by Tan *et al.*,¹⁶ the CP and MP can be estimated from statistical associating fluid theory (SAFT1) that captures the behavior of the corresponding homopolymers. Such mean-field theories cannot account for detailed micelle structure, but can capture the onset of micelle formation, for example on the basis of a nanophase separation hypothesis. While all these results showed in general that that NCM can be used to form micelles, the results were for model copolymers that are not directly applicable to drug delivery.

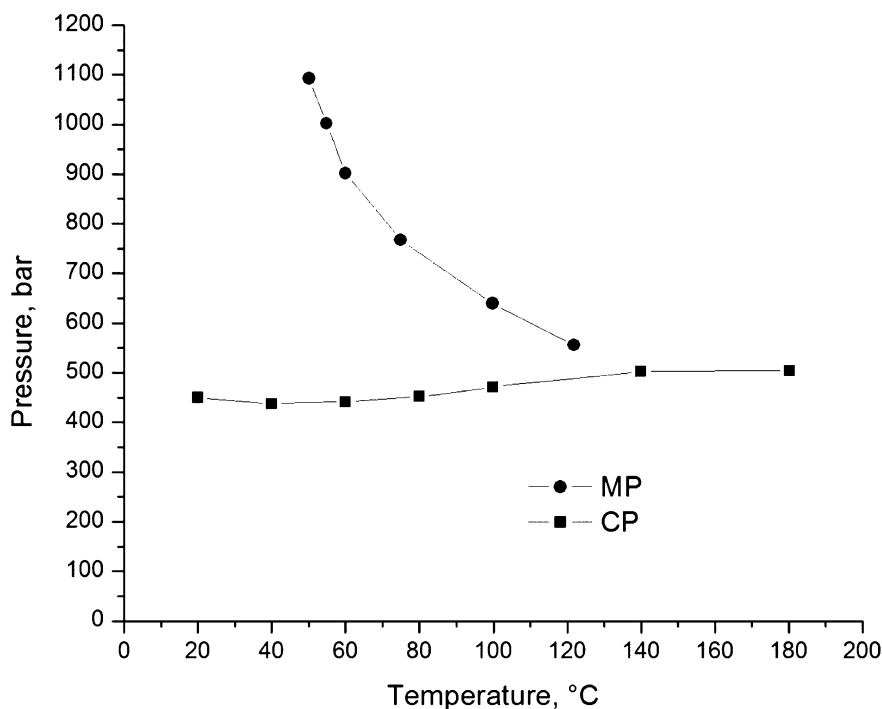


Figure 13.6 Pressure-temperature phase diagram of polystyrene-*block*-polyisoprene (11.5k-*b*-10.5k) in near-critical propane. The concentration of polymer in solution was 0.5 wt%. Re-plotted on the basis of data taken from Winoto *et al.*¹³

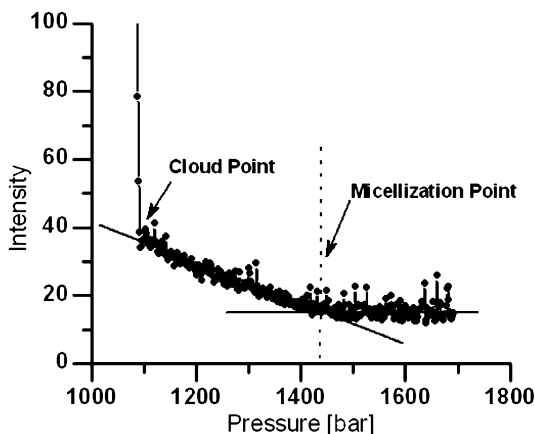


Figure 13.7 Scattered light intensity graph showing micelle formation. This is for PEG-*b*-PCL (5k-*b*-2.3k) in near-critical trifluoromethane at 100 °C and 5 wt%. (Reproduced from Tyrrell *et al.*¹⁸ with permission from the American Chemical Society.)

13.3 Extension to PEG-*b*-PCL

Therefore, the next logical step in developing NCM was to extend it to a biomedically relevant polymer, such as poly(ethylene glycol)-*block*-poly(ϵ -caprolactone),¹⁷ selected for NCM studies by Tyrrell *et al.*¹⁸ Poly(ethylene glycol) (PEG) is a common hydrophilic corona-forming block while poly(ϵ -caprolactone) (PCL) is a common hydrophobic core-forming block; both are biodegradable and FDA approved.

Tyrrell *et al.*¹⁸ chose chlorodifluoromethane and trifluoromethane as possible solvents for NCM, based on polarity and critical properties. While chlorodifluoromethane showed no micellization (due to narrow difference in block CPs), trifluoromethane exhibited evidence of micelle formation, as shown in Figure 13.7. A compilation of the CP and MP results shown in Figure 13.8 confirms a robust micellar region for trifluoromethane.

However, such micelles formed at high pressure may in principle undergo a structural rearrangement or decomposition upon decompression. So, the next step was to confirm that micelles still exist upon dispersion of the copolymer precipitate in water. Towards this end, the solvent was removed from the NCM system depicted in Figure 13.8 by depressurization, and the precipitate was re-dispersed in water and then filtered through a 200 μm filter. The filtered solution was then characterized for particle size. As shown in Figure 13.9, the particle size distribution is narrow and centered around 100 nm, reminiscent of micelle structure in the NCM solution. This was in sharp contrast to a control solution (copolymer dissolved in water without NCM treatment), which could not be dissolved at all.

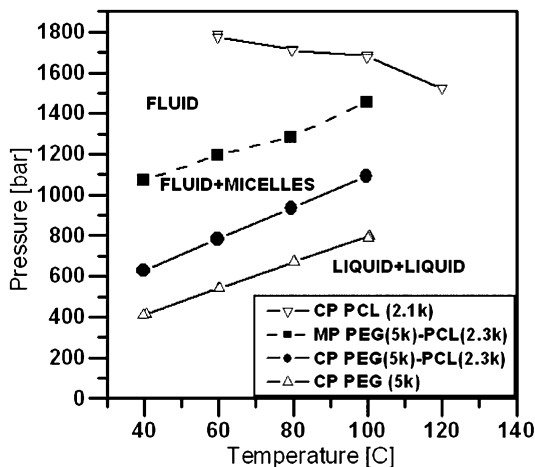


Figure 13.8 Pressure-temperature phase diagram of PEG (5k), PCL (2.3k), and the corresponding block copolymer in near-critical trifluoromethane. The concentrations of polymer were 1 wt% for the homopolymers and 5 wt% for the copolymer. (Reproduced from Tyrrell *et al.*¹⁸ with permission from the American Chemical Society.)

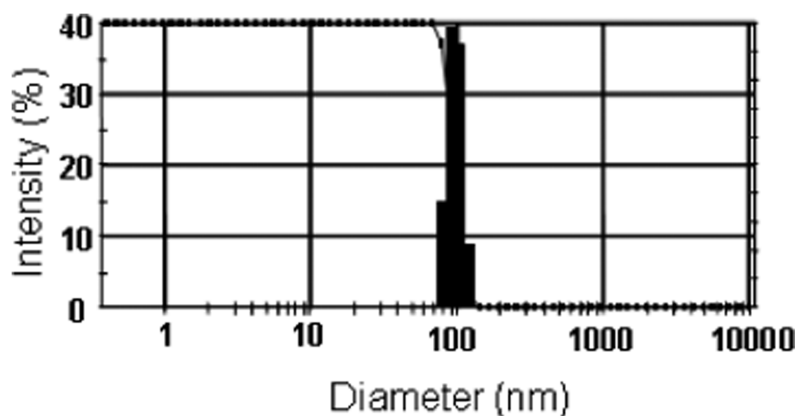


Figure 13.9 Particle size results of PEG-*b*-PCL (5k-*b*-2.3k) in water after near-critical trifluoromethane processing ($P = 650$ bar, $T = 35$ °C). The approximate concentration of polymer in water was ~ 0.1 wt%. The nominal average diameter over three runs was 101 ± 5 nm. (Reproduced from Tyrrell *et al.*¹⁸ with permission from the American Chemical Society.)

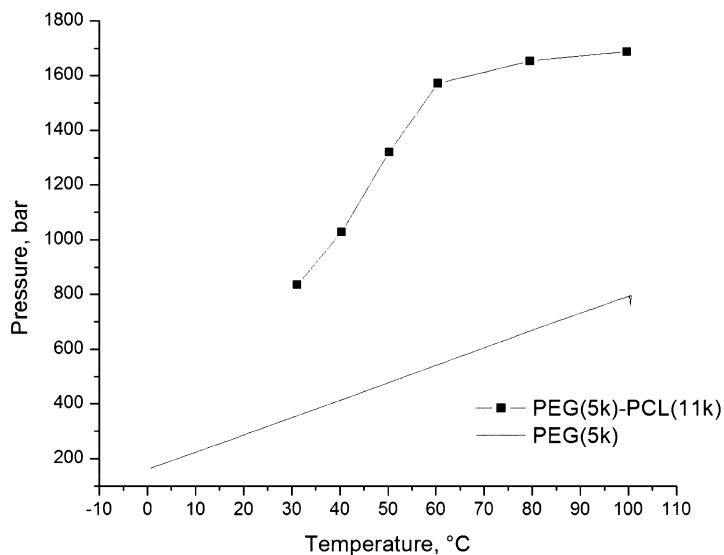


Figure 13.10 Cloud pressures for PEG (5k) and the corresponding PCL block copolymer (5k-*b*-11k) in near-critical trifluoromethane. The concentration of polymer in solution was 1 wt%. Note: micelles are present above the copolymer CP to over 1800 bar (the actual MP was beyond the experimental pressure range). Re-plotted on the basis of data from Green *et al.*¹⁹

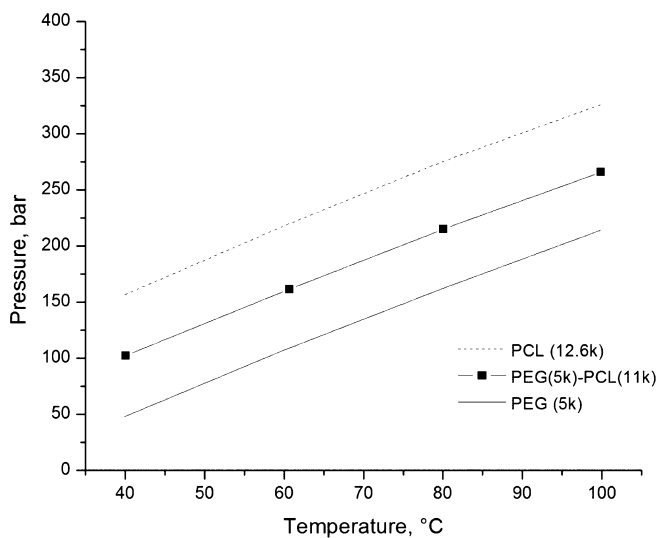


Figure 13.11 Cloud pressures for PEG (5k), PCL (12.6k), and the corresponding block copolymer (5k-*b*-11k) in near-critical dimethyl ether. The concentration of polymer in solution was 1 wt%. Note: micelles were formed at a concentration of 2 wt% for a small region at lower temperatures. Re-plotted on the basis of data from Green *et al.*¹⁹

Figures 13.7–13.9 illustrate that NCM can produce polymeric micelles that are recoverable in water and hence can be potentially useful for drug delivery. However, the phase behavior of that early prototype system was not very practical due to relatively high pressures. Thus, the next objective was to understand how to reduce the NCM pressure, for example, by optimizing the solvent composition effects.

13.4 Optimizing the NCM Solvent

To address this challenge, Green *et al.*¹⁹ chose trifluoromethane, 1,1,1,2-tetrafluoroethane, hexafluoroethane, and dimethyl ether as model solvents, and PEG-*b*-PCL as a model solute, in which the PCL block was substantially larger than that used in the previous figures. Figure 13.10 illustrates sample results for trifluoromethane, in which micelles are found above the CP curve (the actual MP is beyond the pressure limit). Figure 13.11 illustrates that a new solvent, dimethyl ether, is not selective enough for PEG-*b*-PCL to form

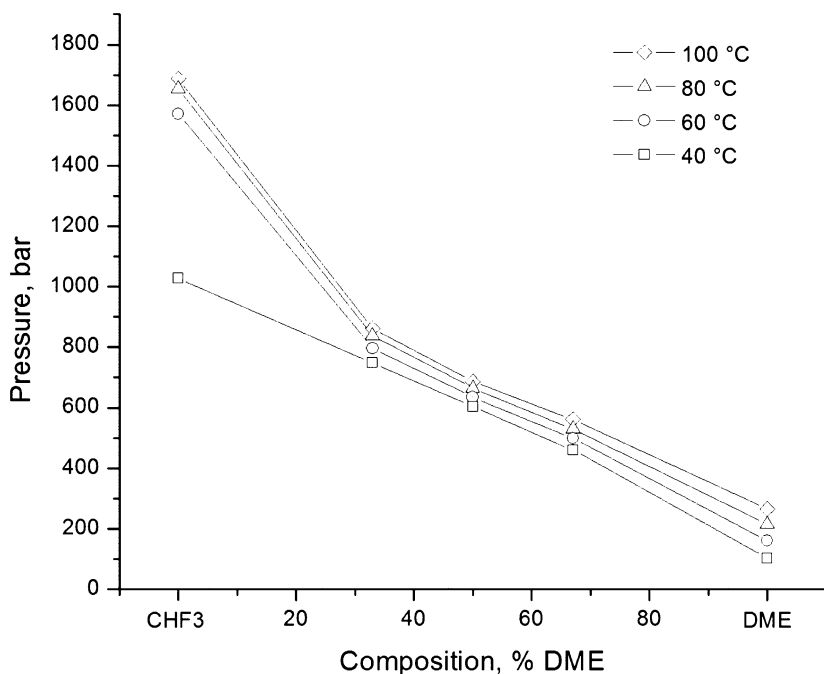


Figure 13.12 Pressure–composition phase diagram for PEG-*b*-PCL (5k-*b*-11k) in near-critical mixtures of trifluoromethane and dimethyl ether at various temperatures. The concentration of polymer in solution was 1 wt%. (Reproduced from Green *et al.*¹⁹ with permission from the American Chemical Society.)

micelles (at this concentration), but the CPs in dimethyl ether are substantially lower than those in trifluoromethane. Hexafluoroethane was found too weak to dissolve the copolymer. While tetrafluoroethane dissolved the copolymer, it did not produce micelles.

These two figures are useful to approximate the solvent capacity and selectivity, which are usually defined in terms of mole or weight fractions. Capacity is a measure of the affinity of the solvent for the polymer. For a given solvent, the capacity roughly scales with density and hence increases with increasing pressure. Therefore, in comparing two different solvents, the one with a lower CP for a given polymer is deemed to have a higher capacity. For example, considering the difference in CP, dimethyl ether should have a higher capacity for the diblock than trifluoromethane due to a much lower CP. Selectivity is a measure of the affinity of a given solvent for one polymer over another. So, for the same solvent, a large difference in CP for two polymers means a high selectivity. Therefore, when the polymers are joined in a

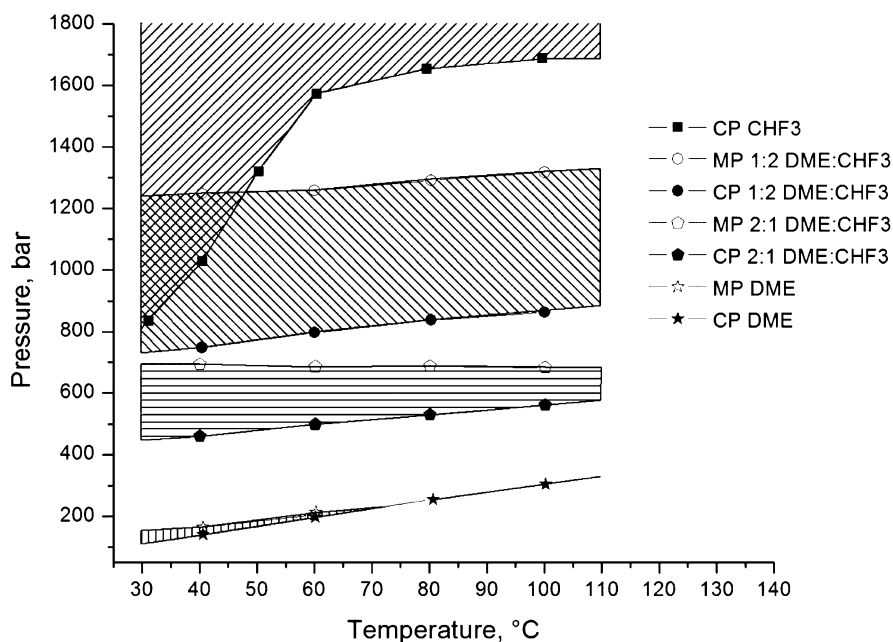


Figure 13.13 Pressure-temperature phase diagram of PEG-*b*-PCL (5k-*b*-11k) in near-critical trifluoromethane, dimethyl ether, and mixtures. Micellar regions are the shaded regions between the CP and MP curves. Note: the upper limit of the shaded region for pure trifluoromethane is the experimental boundary, not the MP. The concentration of polymer in solution was 1 wt% for all but the pure dimethyl ether, which was 2 wt%. (Reproduced from Green *et al.*¹⁹ with permission from the American Chemical Society.)

diblock, high selectivity means a high likelihood of micelle formation. If the solvent is selective enough, the less soluble blocks (high-CP) are induced to precipitate, and form the core of micelles, while the more soluble blocks (low-CP) form the corona. As shown in Figures 13.10 and 13.11, PEG has a low CP in trifluoromethane, while PCL has a very high one (above the experimental range). This means trifluoromethane has high selectivity and high likelihood of micelle formation with PEG-*b*-PCL, which is indeed the case. However, in dimethyl ether, the difference between the two homopolymer CPs is small, which means low selectivity and low probability of micelle formation.

In fact, dimethyl ether did not produce micelles at 1 wt%, but it did at 2 wt% in a small low-temperature region. More important, dimethyl ether exhibited much lower CPs, which suggests a high capacity for PEG-*b*-PCL. This suggested combining the high selectivity of trifluoromethane with the high capacity of dimethyl ether simply by mixing the two pure solvents. Figure 13.12 shows that mixing the two solvents produced a nearly linear

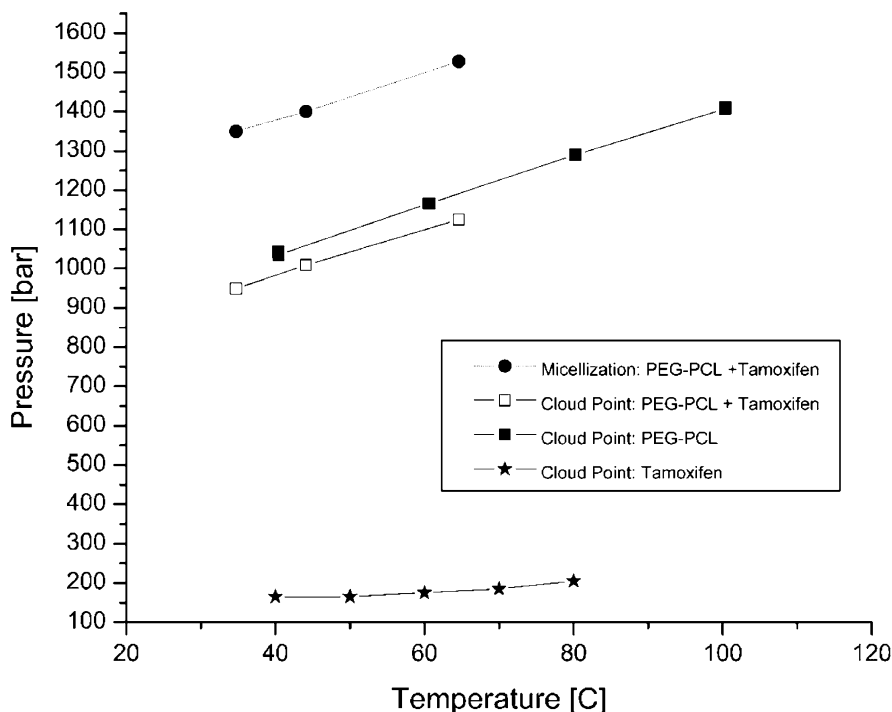


Figure 13.14 Cloud pressures of tamoxifen, PEG-*b*-PCL (5k-*b*-5k), and mixture and micellization pressure of PEG-*b*-PCL (5k-*b*-5k) in near-critical trifluoromethane. The concentrations of polymer and drug in solution are 1 and 0.1 wt%, respectively. (Reproduced from Tyrrell *et al.*²⁰ with permission from the American Chemical Society.)

CP (and hence the capacity) dependence on the amount of dimethyl ether present. Also, as depicted in Figure 13.13, the size of the micellar region scales nicely with solvent composition.

These results serve to show that using mixed solvents allows not only reduction of the operating pressure, but also gives better control over the solvent selectivity and capacity. While these results illustrate an improved NCM control, the next development hurdle was to demonstrate that NCM can be used to make drug-loaded micelles. If so, can NCM allow for improved drug loading?

13.5 Loading PEG-*b*-PCL with a Cancer Drug

Towards this end, Tyrrell *et al.*²⁰ investigated PEG-*b*-PCL (5k-*b*-5k) with tamoxifen in trifluoromethane. An example of their results is shown in Figure 13.14. The CP of the drug is lower than that of the copolymer, which

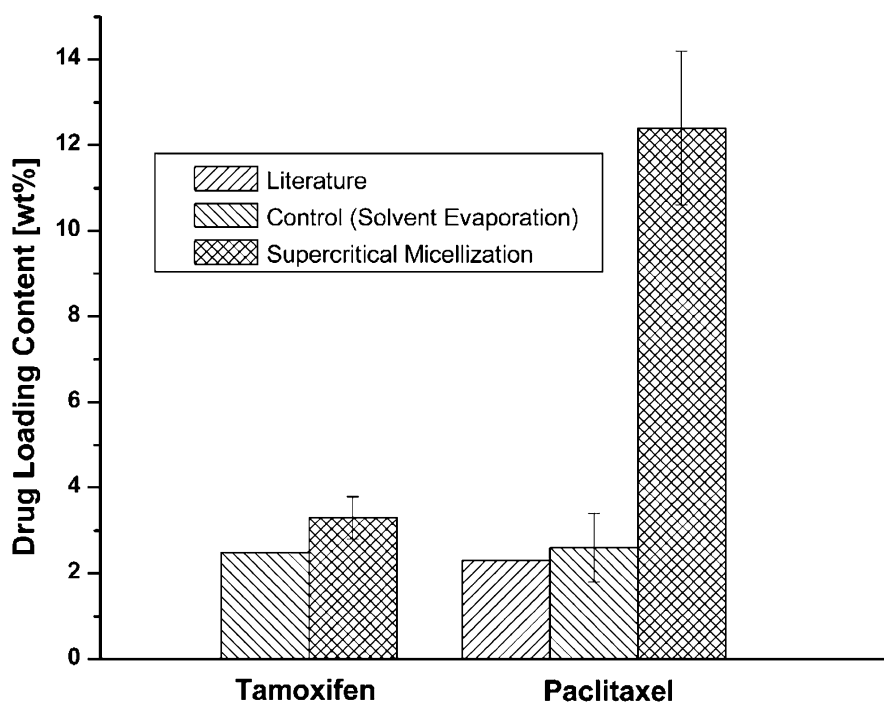


Figure 13.15 Drug loading content of tamoxifen and paclitaxel in PEG-*b*-PCL (5k-*b*-5k). Error bars represent the standard deviation of $n = 3$ for tamoxifen and $n = 5$ for paclitaxel. Literature values for paclitaxel²² were obtained by a solvent evaporation method using THF. A literature reference was unavailable for tamoxifen in PEG-*b*-PCL. (Reproduced from Tyrrell *et al.*²⁰ with permission from the American Chemical Society.)

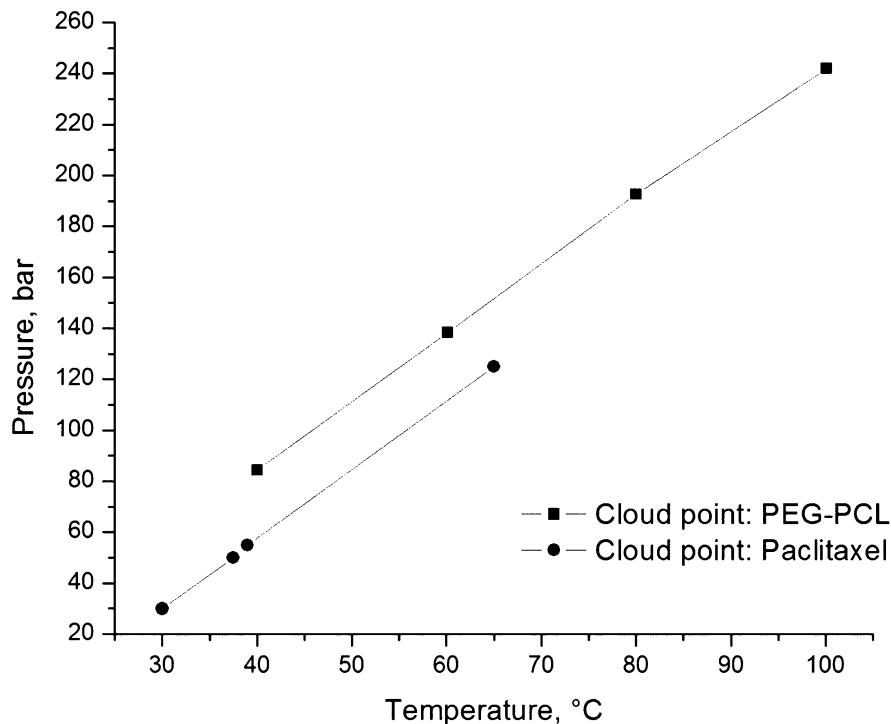


Figure 13.16 Cloud pressures of paclitaxel and PEG-*b*-PCL (5k-*b*-5k) in near-critical dimethyl ether. The concentrations of polymer and drug in solution are 1 and 0.3 wt%, respectively.

implies that the drug is still likely to be in solution when the polymer is precipitated. This leads to a low driving force for the drug to enter into the micelle core. As expected from this low driving force, the corresponding drug loading is about 3.3%, as shown in Figure 13.15 on the left, which is slightly higher than that obtained from the conventional solvent evaporation method.

However, what would happen if the drug CP fell between the MP and the CP of the polymer? As it turns out, paclitaxel satisfies this requirement with PEG-*b*-PCL (5k-*b*-5k). Since paclitaxel does not dissolve in trifluoromethane but easily dissolves in dimethyl ether, as shown in Figure 13.16, their mixture (70% dimethyl ether) allows us to bring the drug CP to the desired pressure range, between the copolymer CP and MP, as shown in Figure 13.17.

As a result, the drug precipitates from solution while micelles are present, which should drive it to the micelle core. This higher driving force results in a much higher drug-loading content, about 12.4%, as is seen from Figure 13.15 on the right. This is a substantial improvement over conventional solvent evaporation, which yields about 2.6% drug-loading content. However, the drug release profile, as seen in Figure 13.18, still exhibits burst release

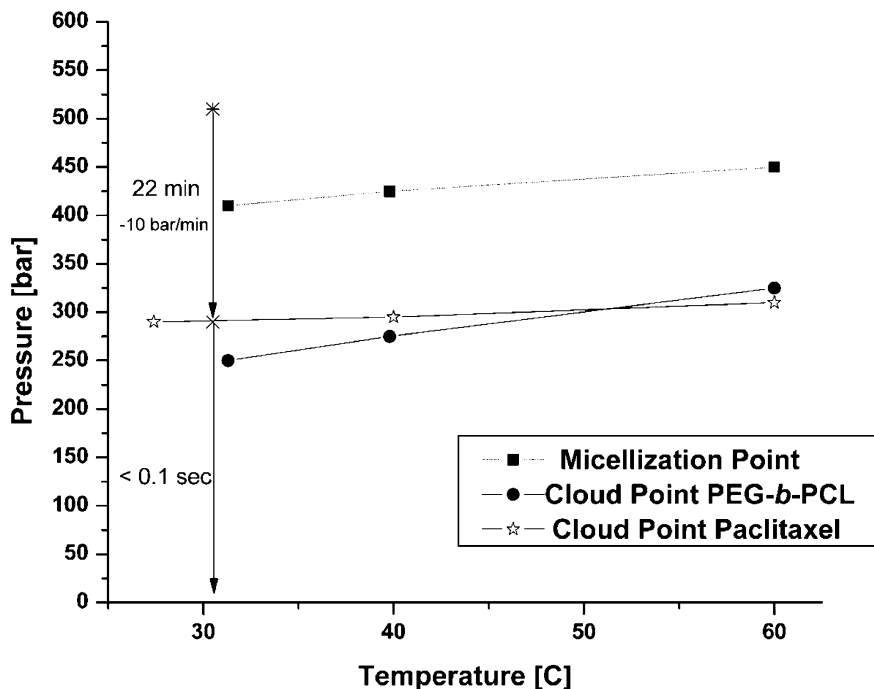


Figure 13.17 Cloud pressures of paclitaxel, PEG-*b*-PCL (5k-*b*-5k), and mixture and micellization pressure (MP) of PEG-*b*-PCL (5k-*b*-5k) in near-critical dimethyl ether/trifluoromethane (70/30) mixture. The concentrations of polymer and drug in solution are 1.5 and 0.15 wt%, respectively. The *arrows* indicate the pressure/time profile of the micellization/depressurization process used to recover drug-loaded micelles. (Reproduced from Tyrrell *et al.*²⁰ with permission from the American Chemical Society.)

characteristic of conventional approaches, which posed a new challenge for NCM.

13.6 NCM: A Remedy for Burst Release?

Tyrrell *et al.*²¹ attempted to address this burst release challenge using a triblock copolymer. A simplistic idea underpinning the conventional methods is that, when diblock micelles are formed in liquid solution, all the drug will be encapsulated in the core of the micelle due to the core-forming block's higher affinity for the drug. As suggested by Tyrrell *et al.*,²¹ for all such conventional methods, much of the drug can be deposited on the outside of the core, which can lead to burst release.

By contrast, a triblock micelle, if made synchronously with drug precipitation, forms a middle layer that can coat and hence protect the

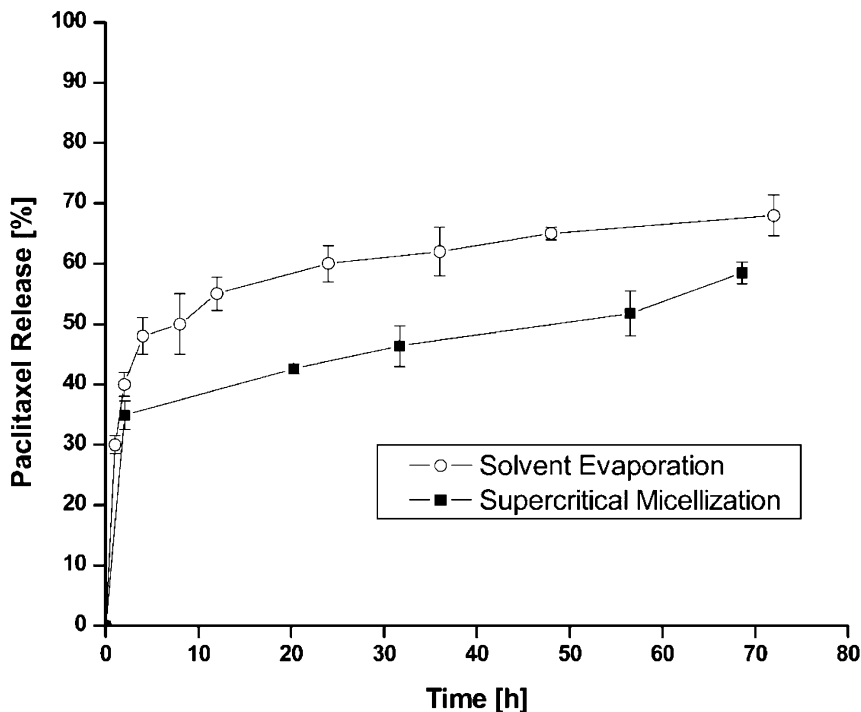


Figure 13.18 Paclitaxel release from PEG-*b*-PCL micelles prepared by solvent evaporation (*open circles*) and supercritical micellization (*squares*) into distilled water at pH = 7.4 and $T = 37^\circ\text{C}$. Error bars represent the standard deviation of $n = 4$ experiments. (Reproduced from Tyrrell *et al.*²⁰ with permission from the American Chemical Society.)

drug that failed to penetrate the core. This would require a sequential collapse of blocks, which in turn requires a control of the phase behavior that is simply unavailable by conventional methods, but attainable by the NCM method.

Tyrrell *et al.*²¹ chose to prove this concept using FDA-approvable blocks, such as corona-forming PEG, core-forming PCL, and middle-layer-forming poly(L-lactic acid) (PLLA) or poly(D,L-lactic acid) (PDLLA) or a random copolymer of PLLA and PDLLA. Figure 13.19 suggests that trifluoromethane has a much lower capacity for PCL than for any of the other homopolymers. In the temperature range of interest, 20–60 °C, PLLA has a CP above that of PEG, and PDLLA has a CP below PEG. So, if the triblock were to consist of a PEG block (to form the corona in water), a PCL block (to form the core), and a middle block of PLLA, a sequential collapse may be viable.

Such a sequential collapse is illustrated in Figure 13.20. The top plot for PEG-*b*-(PCL-*co*-PDLLA) displays only two transitions: one from homogenous to

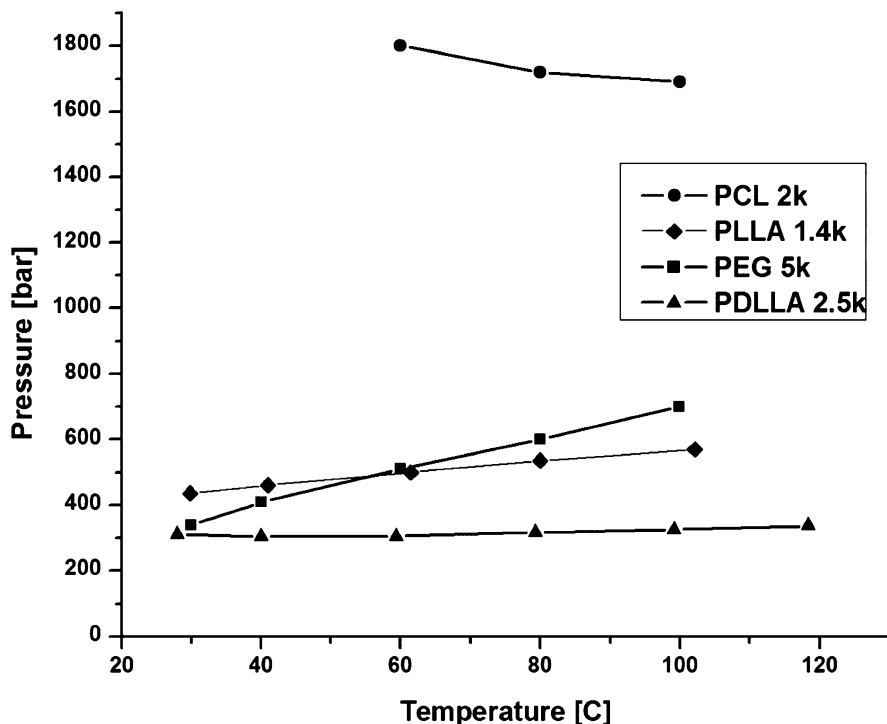


Figure 13.19 Cloud pressures of PCL, PLLA, PEG, and PDLLA in trifluoromethane. The concentrations in solution are 1 wt%. (Reproduced from Tyrrell *et al.*²¹ with permission from the American Chemical Society.)

micellar solution, and one from micellar to bulk precipitation, as expected for a diblock. The bottom plot for the PEG-*b*-PLLA-*b*-PCL triblock shows three distinct transitions. The first transition is from homogenous to micellar state, due to PCL aggregation. The second transition is from the micellar to another micellar state, due to PLLA collapse onto the PCL core. The final one is from micellar to bulk precipitation, due to micelle aggregation. These results for all temperatures are summarized in Figure 13.21. The solvent composition was chosen such that the drug CP fell between the micellization and middle block collapse pressures. Figure 13.22 shows that such a sequential block collapse indeed produces particles that exhibit very little, if any, burst release. This confirms the hypothesis that a precise control of block collapse and drug aggregation, which is virtually impossible with conventional preparation methods but attainable with the NSM method, can indeed produce particles made of FDA-approved blocks that exhibit not only high drug-loading content and efficiency but also burst-free release.

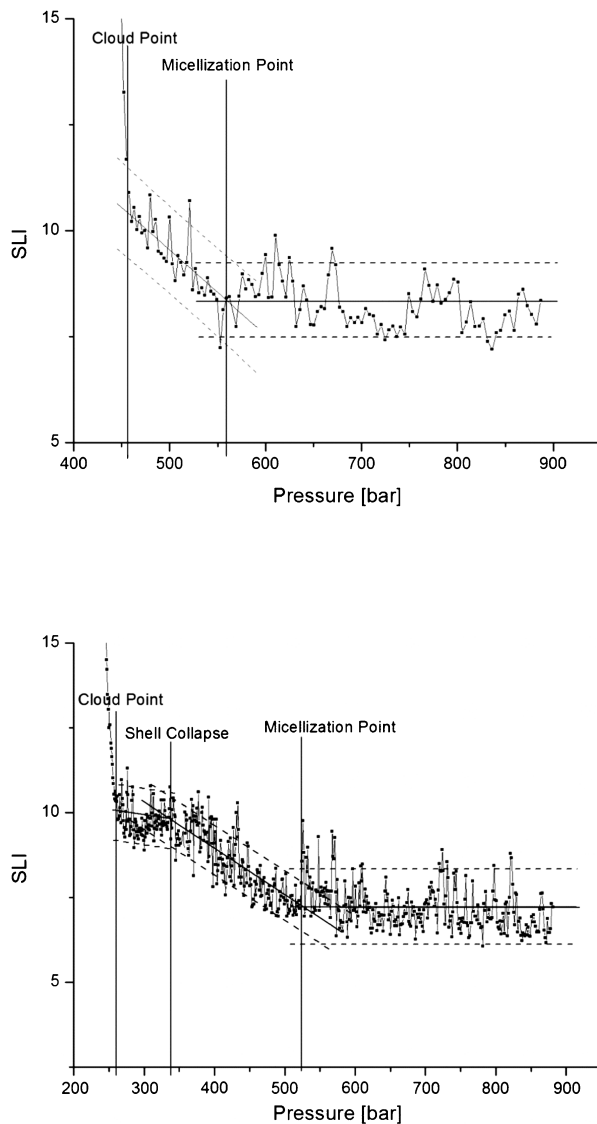


Figure 13.20 Scattered light intensity as a function of pressure for PEG-*b*-(PDLLA-*co*-PCL) [5k-*b*-(2k-*co*-3k)] (*top plot*) and PEG-*b*-PLLA-*b*-PCL (5k-*b*-1.5k-*b*-1.5k) (*bottom plot*). Both are in a 1:1 mix of trifluoromethane/dimethyl ether solution at 40 °C and polymer concentrations of 2 wt%. (Reproduced from Tyrrell *et al.*²¹ with permission from the American Chemical Society.)

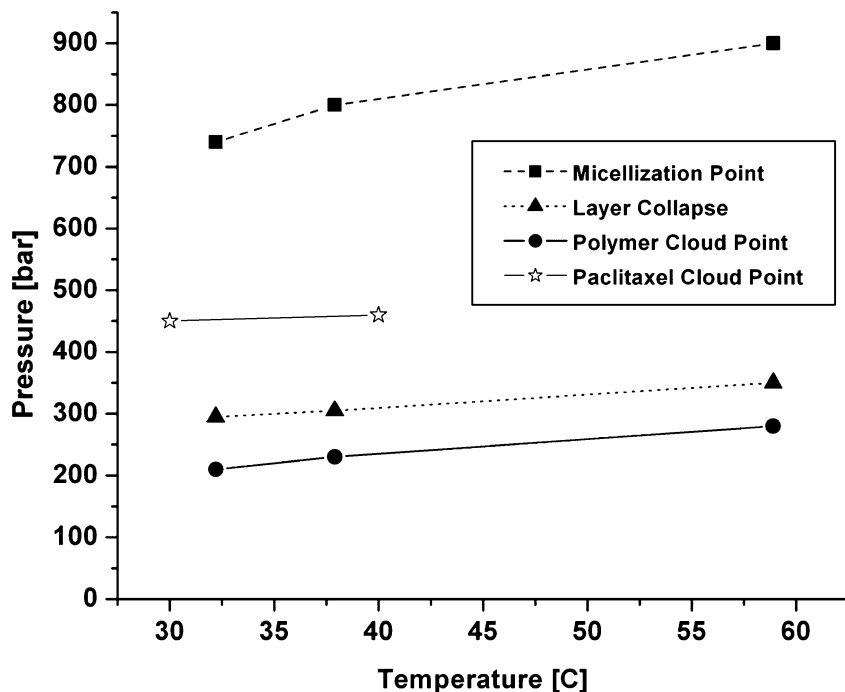


Figure 13.21 Cloud pressure and micellization pressure of PEG-*b*-PLLA-*b*-PCL (5k-*b*-1.5k-*b*-1.5k) and CP of paclitaxel in a 1:1 mix of trifluoromethane/dimethyl ether. Polymer and drug concentrations were 1.5 wt% and 0.15 wt%, respectively. (Reproduced from Tyrrell *et al.*²¹ with permission from the American Chemical Society.)

13.7 Conclusion and Future Research Questions

Near-critical micellization (NCM) can produce solvent-free polymeric micelles useful for drug delivery systems. The NCM-made PEG-*b*-PCL micelles were found not only to be dispersible in water, but also to have drug loading content up to six times higher than that attainable from conventional methods. Even more promising, NCM has been demonstrated to produce sequentially collapsed triblock copolymer micelles, which is impossible to accomplish using conventional methods. Such triblock micelles, made of PEG-*b*-PLLA-*b*-PCL loaded with paclitaxel encapsulated by the middle PLLA layer, were found to exhibit virtually no burst release that is typical of diblock copolymer micelle formulations, while retaining the enhanced drug loading content and drug loading efficiency (Table 13.1).

These early NCM results are promising, but there are many intriguing research questions still to be answered. For example, how to further increase the drug loading by optimizing the process conditions and multi-block structure? How to probe the micelle structure *in situ* at high pressures? How to

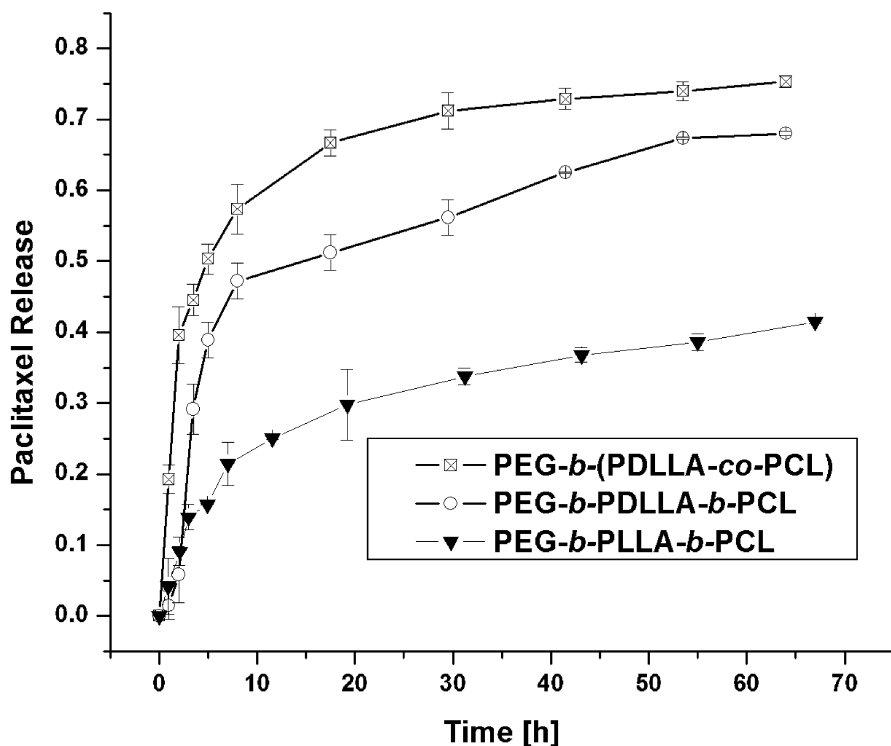


Figure 13.22 Cumulative paclitaxel release from a diblock, PEG-*b*-(PDLLA-*co*-PCL) [5k-*b*-(2k-*co*-3k)], and two triblocks, PEG-*b*-PDLLA-*b*-PCL (5k-*b*-1.5k-*b*-1.5k) and PEG-*b*-PLLA-*b*-PCL (5k-*b*-1.5k-*b*-1.5k), in distilled water at pH = 7.4 and $T = 37^\circ\text{C}$. (Reproduced from Tyrrell *et al.*²¹ with permission from the American Chemical Society.)

extend this method to other polymer–drug formulations? How to scale-up NCM safely to kilogram or more product quantities? How to achieve a consistently uniform product quality necessary for FDA approvals?

Table 13.1 Drug loading and efficiency of diblock and triblock copolymers.^a

Polymer	MW	Loading content	Encapsulation efficiency	Overall loading efficiency
PEG- <i>b</i> -PCL	5k-5k	12.4%	82.1%	87.0%
PEG- <i>b</i> -(PDLLA- <i>co</i> -PCL)	5k-(2k- <i>co</i> -3k)	10.5%	100.0%	80.2%
PEG- <i>b</i> -PDLLA- <i>b</i> -PCL	5k-1.5k-1.5k	10.9%	106.0%	72.3%
PEG- <i>b</i> -PLLA- <i>b</i> -PCL	5k-1.5k-1.5k	10.4%	98.6%	77.1%

^aData shown taken from work by Tyrrell *et al.*^{20,21}

Acknowledgements

The authors would like to acknowledge financial support from the U.S. National Science Foundation (CBET-0828472 and CBET-1034530) and the National Science Foundation of China Distinguished Young Scholar Award (50888001).

References

1. A. V. Kabanov and V. Y. Alakhov, *Amphiphilic Block Copolymers: Self-Assembly and Applications*, Elsevier, Amsterdam, 1997.
2. K. Kataoka, G. Kwon, M. Yokoyama, T. Okano and Y. Sakurai, *J. Controlled Release*, 1992, **24**, 119.
3. T. Koga, S. Zhou, B. Chu, J. L. Fulton, S. Yang, C. K. Ober and B. Erman, *Rev. Sci. Instrum.*, 2001, **72**, 2679.
4. G. Kwon, M. Naito, M. Yokoyama, T. Okano, Y. Sakurai and K. Kataoka, *J. Controlled Release*, 1997, **48**, 195.
5. S. B. La, T. Okano and K. Kataoka, *J. Pharm. Sci.*, 1996, **85**, 85.
6. G. Kwon, *Crit. Rev. Ther. Drug Carrier Syst.*, 2003, **20**, 357–301.
7. V. Torchilin, *J. Controlled Release*, 2001, **73**, 137–172.
8. Z. Tyrrell, Y. Shen and M. Radosz, *Prog. Polym. Sci.*, 2010, **35**, 1128–1143.
9. G. Gaucher, M.-H. Dufresne, V. Sant, N. Kang, D. Maysinger and J.-C. Leroux, *J. Controlled Release*, 2005, **109**, 169–188.
10. R. Gref, Y. Minamitake, M. Peracchia, V. Trubetskoy, V. Torchilin and R. Langer, *Science*, 1994, **263**, 1600–1603.
11. P. Vangeyte, S. Gautier and R. Jérôme, *Colloids Surf., A*, 2004, **242**, 203–211.
12. J. L. Kendall, D. A. Canelas, J. L. Young and J. M. DeSimone, *Chem. Rev.*, 1999, **99**, 543–563.
13. W. Winoto, H. Adidharma, Y. Shen and M. Radosz, *Macromolecules*, 2006, **39**, 8140–8144.
14. A. K. C. Chan, P. Russo and M. Radosz, *Fluid Phase Equilib.*, 2000, **173**, 149.
15. M. Łuszczuk and M. Radosz, *J. Chem. Eng. Data*, 2003, **48**, 226–330.
16. S. Tan, W. Winoto and M. Radosz, *J. Phys. Chem. C*, 2007, **111**, 15752–15758.
17. C. Allen, Y. Yu, D. Maysinger and A. Eisenburg, *Bioconjugate Chem.*, 1998, **9**, 564–572.
18. Z. Tyrrell, W. Winoto, Y. Shen and M. Radosz, *Ind. Eng. Chem. Res.*, 2009, **48**, 1928–1932.
19. J. Green, Z. Tyrrell and M. Radosz, *J. Phys. Chem. C*, 2010, **114**, 16082–16086.
20. Z. Tyrrell, Y. Shen and M. Radosz, *J. Phys. Chem. C*, 2011, **115**, 11951–11956.
21. Z. Tyrrell, Y. Shen and M. Radosz, *Macromolecules*, 2012, **45**, 4809–4817.
22. X. Shuai, T. Merdan, A. Schaper, F. Xi and T. Kissel, *Bioconjugate Chem.*, 2004, **15**, 441–448.